

Reaction of arsane with cobalt or iron carbonyls, and the X-ray crystal structures of $[\text{Fe}_2(\text{CO})_8(\mu_4\text{-As})]_2[\text{Fe}_2(\text{CO})_6]$ and $[\mu_4\text{-AsCo}_3(\text{CO})_8]_3$

Leslie J. Arnold, Kenneth M. Mackay * and Brian K. Nicholson *

School of Science, University of Waikato, Private Bag, Hamilton, (New Zealand)

(Received November 14th, 1989)

Abstract

Reaction of AsH_3 with $\text{Fe}(\text{CO})_5$ in a hydrocarbon solvent at 110°C provides an improved route to $(\mu_3\text{-As})_2\text{Fe}_3(\text{CO})_9$, while the corresponding reaction at 70°C with $\text{Fe}_2(\text{CO})_9$ has given the new cluster $[\text{Fe}_2(\text{CO})_8(\mu_4\text{-As})]_2[\text{Fe}_2(\text{CO})_6]$, which has been shown by X-ray crystallography to consist of four AsFe_2 triangles linked by *spiro*-As atoms and an Fe–Fe edge. The reaction at 20°C of AsH_3 with $\text{Co}_2(\text{CO})_8$ gave the known trimer $[\mu_4\text{-AsCo}_3(\text{CO})_8]_3$ which was fully characterised by an X-ray diffraction study.

Introduction

We have previously investigated the reactions of the hydrides EH_4 ($\text{E} = \text{Si}, \text{Ge}, \text{or Sn}$) with cobalt and iron carbonyls, and have shown that a range of interesting mixed-metal clusters is accessible through such reactions [1,2]. The reactions involve cleavage of the relatively weak E–H bonds to give E–M bonds with elimination of H_2 , and subsequent rearrangements lead to clusters. In reactions with the heavier group 15 organo-hydrides $\text{R}_n\text{E}'\text{H}_{3-n}$ ($\text{E}' = \text{P}, \text{As}$) the E'–H bond can also be transformed into an E'–M bond [3], but there appears to have been little previous work on the use of the parent arsenic hydride, AsH_3 , in cluster synthesis; the only other study of which we are aware was described in a conference paper on arsenic-osmium clusters [4]. The As–H bond strength (247 kJ mol^{-1}) is similar to that of a Sn–H bond (252 kJ mol^{-1}) and weaker than that of a Ge–H bond (290 kJ mol^{-1}) [5] and so we would expect reactions to take place under similar conditions to those established for the heavier group 14 hydrides.

Two excellent reviews are available summarising the general area of mixed main-group/transition metal clusters [6].

We now report the formation of As–Co and As–Fe clusters via the hydride route; one new species is described and some known species have been prepared in

better yields than those previously reported. The structure of $[\text{Fe}_2(\text{CO})_8(\mu_4\text{-As})]_2[\text{Fe}_2(\text{CO})_6]$ (**2**) and $[\mu_4\text{-AsCo}_3(\text{CO})_8]_3$ (**3**) are described.

Experimental

The inert atmosphere techniques and equipment have been described elsewhere [1,2]. AsH_3 was prepared by a variation of the procedure given in Inorganic Syntheses [7], involving addition of sulphuric acid to a basic solution of As_2O_3 and KBH_4 . The apparatus used was similar to that previously described [7], but the evolved gases were dried by passing through columns packed with calcium chloride and sodium hydroxide before traps at -22 , -96 and -196°C , with pure AsH_3 condensing in the final one. Purity was checked by an infrared spectrum [7]. [Caution: AsH_3 is very toxic, Surplus arsane can be destroyed by condensing it on to a solution of Br_2 in hexane and allowing the mixture to warm up slowly.]

Reaction of AsH_3 with $\text{Fe}(\text{CO})_5$. AsH_3 (0.5 mmol), $\text{Fe}(\text{CO})_5$ (2 ml, 14.9 mmol) and light petroleum ether (5 ml, $100\text{--}130^\circ\text{C}$ fraction) were sealed in a glass ampoule (ca. 50 ml), which was then placed inside a steel pressure vessel and kept at 110°C for 30 min. The ampoule containing the red mixture was cooled to -196°C and opened to the vacuum line. Incondensable gases were pumped away, the mixture was allowed to warm to room temperature, and the volatile components were removed (solvent, $\text{Fe}(\text{CO})_5$, some AsH_3). The residue was extracted with light petroleum ether ($30\text{--}40^\circ\text{C}$ fraction, 2×5 ml) to give a red solution and then with CH_2Cl_2 (2×5 ml) to give a brown solution. (The remaining black solid contained traces of material soluble in THF or acetone; the THF extract gave weak IR bands at 2052, 2033 and 1959 cm^{-1} .) The red solution was passed through an alumina column (activity III, 2×5 cm), with light petroleum as eluent spirit; this freed it from traces of darker components. The solvent was evaporated to leave $(\mu_3\text{-As})_2\text{Fe}_3(\text{CO})_9$, (**1**) (0.022 g, 15% based on AsH_3). $\nu(\text{CO})$, (hexane), 2037vs, 2006m. The brown dichloromethane solution contained an unidentified species (0.023 g) with $\nu(\text{CO})$ bands at 2080m, 2064vs, 2017w. The reaction was repeated with varying stoichiometries, temperatures, and times, but no higher yields were obtained.

Reaction of AsH_3 with $\text{Fe}_2(\text{CO})_9$. $\text{Fe}_2(\text{CO})_9$ (0.50 g, 1.37 mmol), AsH_3 (1 mmol) and hexane (50 ml) were placed in a flask fitted with a greaseless tap. The mixture was heated with occasional shaking at 70°C for 1 h, to produce a red-brown solution and some unchanged $\text{Fe}_2(\text{CO})_9$. The solvent and some $\text{Fe}(\text{CO})_5$ were pumped away, and the residue was extracted with light petroleum ether. An infrared spectrum of the crude extract showed the presence of minor amounts of $(\mu_3\text{-As})_2\text{Fe}_3(\text{CO})_9$, while the major green product was obtained as black crystals on cooling the extract to -10°C , (75–100 mg, 15–20%). Infrared: $\nu(\text{CO})$ (CH_2Cl_2) 2114w, 2097s, 2066s, 2058w, 2044vs, 1999m, 1967 m cm^{-1} . A FAB mass spectrum showed a peak at m/e 1102 (M^+), and a clear succession of carbonyl-loss peaks to m/e 654 ($M - 16\text{CO}$) $^+$. The compound was fully characterised as $[\text{Fe}_2(\text{CO})_8(\mu_4\text{-As})]_2[\text{Fe}_2(\text{CO})_6]$ (**2**) by a full X-ray crystal structure determination (see below).

Reactions of SbH_3 . SbH_3 was prepared analogously to AsH_3 [7], and was treated in the same way with $\text{Fe}(\text{CO})_5$ at 70 and 105°C , and with $\text{Fe}_2(\text{CO})_9$ and $\text{Fe}_3(\text{CO})_{12}$ at 70°C . In all these cases an antimony mirror was formed and H_2 was evolved. A small proportion of the black residues could be extracted with acetone, and showed a broad $\nu(\text{CO})$ band at 2045 cm^{-1} .

Reaction of AsH₃ with Co₂(CO)₈. AsH₃ (0.81 mmol), Co₂(CO)₈ (0.414 g, 1.21 mmol) and hexane (7 ml) were sealed in an ampoule (ca. 50 ml). The mixture was left in the dark for 1 month. The ampoule was cooled to -196°C and opened to the vacuum line. The gaseous components were CO (2.4 mmol) and H₂ (0.5 mmol). After thawing, the components volatile at room temperature were pumped away and the residue was extracted with a small volume of hexane to remove unchanged Co₂(CO)₈ and some Co₄(CO)₁₂. A subsequent CH₂Cl₂ extraction contained the major product, which was purified by radial chromatography on a Chromatotron (silica plate, hexane as eluent). The first component eluted was a trace of Co₄(CO)₁₂, while the second, major, species was [μ_4 -AsCo₃(CO)₈]₃ (**3**), which was recrystallised from hexane, 0.054 g, 17%, and identified from its infrared spectrum ($\nu(\text{CO})$, hexane, 2073vs, 2063s, 2043m, 2023m, 2016vw, 2009vw) [8,9], and by a crystal structure determination (see below).

X-ray crystallography

For both analyses the space groups were indicated from preliminary precession photography. Intensity data were collected on a Nicolet P3 diffractometer using zirconium-filtered Mo-K α X-rays (λ 0.7107 Å).

*Crystal structure of [Fe₂(CO)₈(μ_4 -As)]₂[Fe₂(CO)₆] (**2**).* Small green-black crystals were obtained from hexane at -10°C ; these did not diffract strongly but provided an adequate data set.

Crystal data: C₂₂As₂Fe₆O₂₂, *M* 1101.15, orthorhombic, space group *Pbca*, *a* 22.908(7), *b* 17.521(9), *c* 16.071(7), *U* 6451(5) Å³. *D_c* 2.28 for *Z* = 8, *F*(000) 4240, $\mu(\text{Mo-K}\alpha)$ 50 cm⁻¹, *T* -100°C , crystal size 0.34 × 0.28 × 0.12 mm. A total of 4529 unique reflections in the range $4^{\circ} < 2\theta < 52^{\circ}$ were collected and corrected for absorption by an empirical method (max, min transmission factors 0.663, 0.572). Of these, 1322 data with $I > 2.5\sigma(I)$ were used in all calculations. The structure was solved by direct methods (SHELXS-86 [10]). In the final cycles of full-matrix least-squares refinement Fe and As atoms were assigned anisotropic temperature factors while the carbonyl groups were refined isotropically. Atoms C(21), C(32), C(33) and O(23) did not refine satisfactorily until their temperature factors were fixed at reasonable values. Refinement converged at *R* = 0.0995, *R_w* = 0.0954 where $w = [\sigma^2(F) + 0.00306F^2]^{-1}$. No parameter showed a final shift more than 0.06σ, and a difference map showed some chemically insignificant peaks of ca. 1.55 e Å⁻³, no doubt arising from problems associated with a weakly diffracting crystal. Final atom coordinates are given in Table 1, and Table 2 gives selected bond parameters. The full structure is illustrated in Fig. 1.

*Crystal structure of [μ_4 -AsCo₃(CO)₈]₃ (**3**).* Green-black needle shaped crystals were obtained from hexane at -30°C .

Crystal data: C₂₄As₃Co₉O₂₄, *M* 1427.413, rhombohedral, space group *R* $\bar{3}$, *a* 40.593(9), *c* 12.766(4) Å, *U* 18217(9) Å³ (hexagonal setting). *D_c* 2.34 for *Z* = 18, *F*(000) 12204. $\mu(\text{Mo-K}\alpha)$ 56.7 cm⁻¹, *T* -100°C , crystal size 0.50 × 0.12 × 0.12 mm.

A total of 5296 unique reflections in the range $4^{\circ} < 2\theta < 45^{\circ}$ were collected and corrected for absorption by an empirical method (max, min transmission factors 0.969, 0.821). Of these 2504 data with $I > 2\sigma(I)$ were used in all calculations. The structure was solved by direct methods (SHELXS-86 [10]) and routinely developed.

Table 1

Final positional parameters for $[\text{Fe}_2(\text{CO})_8(\mu_4\text{-As})]_2[\text{Fe}_2(\text{CO})_6]$ (2)

Atom	x	y	z	Atom	x	y	z
As(1)	0.1790(2)	0.0822(3)	0.3584(3)	C(61)	-0.016(3)	0.237(4)	0.460(4)
As(2)	0.0602(2)	0.1637(3)	0.3182(3)	C(62)	0.004(3)	0.372(3)	0.403(4)
Fe(1)	0.0818(3)	0.0401(4)	0.3616(5)	C(63)	0.096(3)	0.315(4)	0.327(4)
Fe(2)	0.1327(3)	0.1106(4)	0.2325(5)	C(64)	0.091(2)	0.264(3)	0.475(3)
Fe(3)	0.2486(4)	0.1502(4)	0.4438(5)	O(11)	0.041(2)	0.070(2)	0.530(2)
Fe(4)	0.2641(3)	0.0047(4)	0.3831(5)	O(12)	0.383(2)	0.119(3)	0.888(3)
Fe(5)	-0.0326(4)	0.2157(6)	0.2772(6)	O(13)	0.479(2)	0.518(2)	0.730(3)
Fe(6)	0.0399(4)	0.2791(5)	0.3924(6)	O(21)	0.048(2)	0.106(2)	0.096(2)
C(11)	0.058(3)	0.057(4)	0.465(4)	O(22)	0.206(2)	0.235(3)	0.173(3)
C(12)	0.103(3)	-0.055(3)	0.370(4)	O(23)	0.305(1)	0.018(2)	0.655(2)
C(13)	0.016(2)	0.008(3)	0.306(3)	O(31)	0.181(2)	0.109(2)	0.585(2)
C(21)	0.079(2)	0.108(3)	0.154(3)	O(32)	0.363(2)	0.141(3)	0.531(3)
C(22)	0.174(3)	0.190(3)	0.197(3)	O(33)	0.302(2)	0.294(2)	0.790(2)
C(23)	0.167(2)	0.030(3)	0.186(3)	O(34)	0.222(2)	0.190(2)	0.967(3)
C(31)	0.206(3)	0.121(4)	0.524(4)	O(41)	0.204(2)	-0.055(3)	0.531(3)
C(32)	0.317(2)	0.146(3)	0.494(3)	O(42)	0.237(2)	-0.133(2)	0.296(2)
C(33)	0.283(2)	0.180(3)	0.362(4)	O(43)	0.379(2)	-0.029(2)	0.458(3)
C(34)	0.229(3)	0.243(4)	0.457(4)	O(44)	0.318(2)	0.446(2)	0.728(3)
C(41)	0.228(3)	-0.031(4)	0.480(4)	O(51)	0.034(2)	0.307(2)	0.157(3)
C(42)	0.246(3)	-0.079(3)	0.329(3)	O(52)	0.418(2)	0.104(3)	0.114(3)
C(43)	0.334(2)	-0.019(3)	0.429(3)	O(53)	0.382(3)	0.333(4)	0.204(3)
C(44)	0.294(3)	0.041(3)	0.292(4)	O(54)	-0.078(2)	0.125(2)	0.142(3)
C(51)	0.005(3)	0.275(4)	0.205(4)	O(61)	-0.051(2)	0.224(3)	0.511(3)
C(52)	-0.061(4)	0.156(5)	0.354(5)	O(62)	0.486(2)	0.433(2)	0.088(2)
C(53)	-0.079(5)	0.285(7)	0.281(7)	O(63)	0.133(2)	0.350(2)	0.285(2)
C(54)	-0.061(3)	0.161(4)	0.193(4)	O(64)	0.115(2)	0.246(2)	0.039(3)

In the final cycles of full-matrix least-squares refinement Co and As atoms were assigned anisotropic temperature factors while the carbonyl groups were refined isotropically. Refinement converged at $R = 0.0913$, $R_w = 0.0647$ where $w = [\sigma^2(F)]^{-1}$. No parameter showed a final shift more than 0.04σ , and a difference

Table 2

Selected bond parameters for $[\text{Fe}_2(\text{CO})_8(\mu_4\text{-As})]_2[\text{Fe}_2(\text{CO})_6]$ (2)

<i>Bond lengths (Å)</i>			
As(1)–Fe(1)	2.35(1)	As(2)–Fe(1)	2.32(1)
As(1)–Fe(2)	2.339(9)	As(2)–Fe(2)	2.35(1)
As(1)–Fe(3)	2.42(1)	As(2)–Fe(5)	2.41(1)
As(1)–Fe(4)	2.408(9)	As(2)–Fe(6)	2.39(1)
Fe(1)–Fe(2)	2.68(1)	Fe(5)–Fe(6)	2.72(1)
Fe(3)–Fe(4)	2.75(1)		
<i>Non-bonded distances (Å)</i>			
As(1)...As(2)	3.13	O(34)...O(64)	2.872
<i>Angles (°)</i>			
Fe(1)–As(1)–Fe(2)	69.9(3)	Fe(1)–As(2)–Fe(2)	70.0(3)
Fe(3)–As(1)–Fe(4)	69.5(3)	Fe(5)–As(2)–Fe(6)	69.2(3)

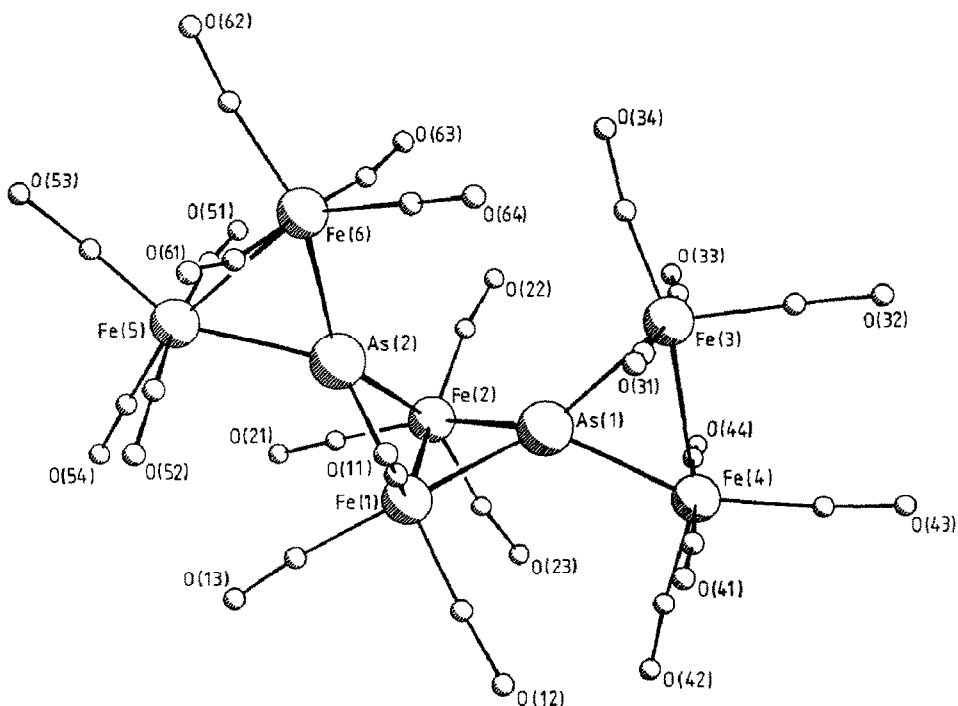


Fig. 1. A PLUTO diagram of the structure of $[\text{Fe}_2(\text{CO})_8(\mu_4\text{-As})]_2[\text{Fe}_2(\text{CO})_6]$ (2).

map showed some chemically insignificant peaks of ca. $1 \text{ e } \text{\AA}^{-3}$, no doubt arising from problems associated with a weakly diffracting crystal and with the absorption correction. Final atom coordinates are given in Table 3, while Table 4 gives selected bond parameters. The full structure is illustrated in the Fig. 2, and Fig. 3 shows the

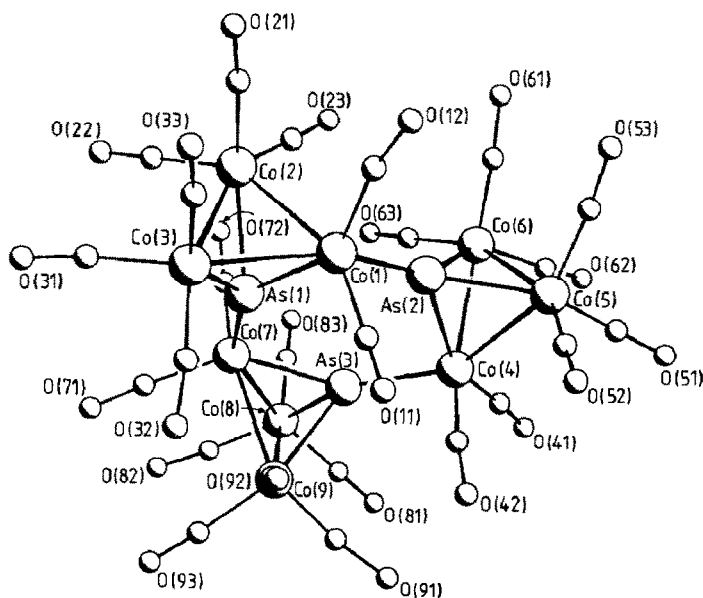


Fig. 2. A view of the full structure of $[\mu_4\text{-AsCo}_3(\text{CO})_9]_3$ (3), showing labelling scheme.

Table 3

Final positional parameters for $[\mu_4\text{-AsCo}_3(\text{CO})_8]_3$ (3)

Atom	x	y	z	Atom	x	y	z
As(1)	0.2194(1)	0.0564(1)	0.5984(2)	C(81)	0.0937(9)	0.0164(9)	0.922(3)
As(2)	0.2548(1)	0.0430(1)	0.8207(2)	C(82)	0.089(1)	−0.037(1)	0.788(3)
As(3)	0.1706(1)	0.0371(1)	0.8245(2)	C(83)	0.074(1)	0.016(1)	0.719(4)
Co(1)	0.2778(1)	0.0733(1)	0.6640(3)	C(91)	0.1560(8)	0.0993(8)	0.902(3)
Co(2)	0.2467(1)	0.0260(1)	0.5123(3)	C(92)	0.2013(9)	0.1175(9)	0.733(2)
Co(3)	0.2662(1)	0.0962(1)	0.4850(3)	C(93)	0.1274(9)	0.0970(9)	0.707(3)
Co(4)	0.2159(1)	0.0452(1)	0.9453(3)	O(11)	0.3050(6)	0.1475(6)	0.756(2)
Co(5)	0.2801(1)	0.0502(1)	0.9856(3)	O(12)	0.3502(7)	0.0744(7)	0.648(2)
Co(6)	0.2250(1)	−0.0118(1)	0.9162(3)	O(21)	0.3145(7)	0.0314(7)	0.409(2)
Co(7)	0.1577(1)	0.0335(1)	0.6511(3)	O(22)	0.1873(6)	−0.0085(6)	0.352(2)
Co(8)	0.1069(1)	0.0123(1)	0.7965(4)	O(23)	0.2216(6)	−0.0415(7)	0.639(2)
Co(9)	0.1561(1)	0.0825(1)	0.7738(3)	O(31)	0.2225(7)	0.0845(7)	0.294(2)
C(11)	0.2942(7)	0.1181(8)	0.721(2)	O(32)	0.2754(6)	0.1717(7)	0.528(2)
C(12)	0.321(1)	0.0720(9)	0.654(3)	O(33)	0.3411(7)	0.1193(7)	0.400(2)
C(21)	0.288(1)	0.0281(9)	0.451(3)	O(41)	0.1710(6)	0.0182(6)	1.136(2)
C(22)	0.2107(9)	0.0047(9)	0.414(3)	O(42)	0.2460(6)	0.1262(6)	0.977(2)
C(23)	0.231(1)	−0.014(1)	0.592(3)	O(51)	0.2640(7)	0.0386(7)	1.211(2)
C(31)	0.2409(9)	0.0893(9)	0.370(3)	O(52)	0.3310(6)	0.1326(6)	0.987(2)
C(32)	0.2725(8)	0.1408(9)	0.516(2)	O(53)	0.3376(7)	0.0277(6)	0.950(2)
C(33)	0.313(1)	0.112(1)	0.438(3)	O(61)	0.2657(7)	−0.0499(7)	0.851(2)
C(41)	0.1891(8)	0.0280(8)	1.061(3)	O(62)	0.2017(7)	−0.0436(7)	1.131(2)
C(42)	0.2319(8)	0.0939(9)	0.960(2)	O(63)	0.1559(7)	−0.0595(7)	0.807(2)
C(51)	0.271(1)	0.043(1)	1.122(3)	O(71)	0.1244(6)	0.0583(6)	0.491(2)
C(52)	0.309(1)	0.099(1)	0.989(3)	O(72)	0.1378(6)	−0.0426(6)	0.580(2)
C(53)	0.315(1)	0.037(1)	0.962(3)	O(81)	0.0859(6)	0.0174(6)	1.010(2)
C(61)	0.249(1)	−0.035(1)	0.875(3)	O(82)	0.0765(7)	0.9312(7)	0.785(2)
C(62)	0.210(1)	−0.030(1)	1.048(3)	O(83)	0.0521(9)	0.0164(9)	0.662(2)
C(63)	0.184(1)	−0.038(1)	0.848(3)	O(91)	0.1590(6)	0.1084(6)	0.988(2)
C(71)	0.1371(9)	0.0485(9)	0.551(2)	O(92)	0.2312(7)	0.1413(7)	0.714(2)
C(72)	0.1431(8)	−0.0127(8)	0.614(2)	O(93)	0.1089(8)	0.1067(7)	0.664(2)

Table 4

Selected bond parameters for $[\mu_4\text{-AsCo}_3(\text{CO})_8]_3$ (3)

<i>Bond lengths (Å)</i>			
As(1)–Co(1)	2.272(5)	As(3)–Co(8)	2.287(5)
As(1)–Co(2)	2.307(5)	As(3)–Co(9)	2.291(5)
As(1)–Co(3)	2.290(5)	Co(1)–Co(2)	2.571(6)
As(1)–Co(7)	2.294(5)	Co(1)–Co(3)	2.599(6)
As(2)–Co(1)	2.290(5)	Co(2)–Co(3)	2.572(6)
As(2)–Co(4)	2.278(5)	Co(4)–Co(5)	2.563(6)
As(2)–Co(5)	2.297(5)	Co(4)–Co(6)	2.547(6)
As(2)–Co(6)	2.281(5)	Co(5)–Co(6)	2.546(6)
As(3)–Co(4)	2.293(5)	Co(7)–Co(8)	2.583(6)
As(3)–Co(7)	2.265(5)	Co(7)–Co(9)	2.558(6)
<i>Bond angles (°)</i>			
Co(1)–As(1)–Co(7)	141.0(2)	As(1)–Co(1)–As(2)	94.4(2)
Co(1)–As(2)–Co(4)	134.0(2)	As(2)–Co(4)–As(3)	92.6(2)
Co(4)–As(3)–Co(7)	144.2(2)	As(1)–Co(7)–As(3)	95.2(2)

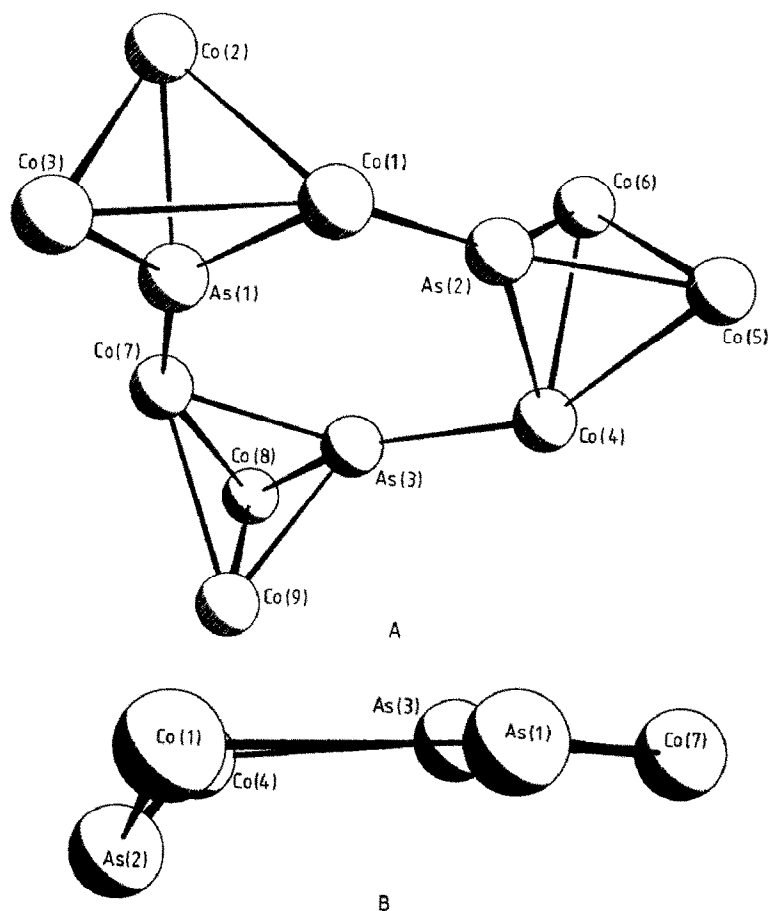


Fig. 3. (a) The metal skeleton of $[\mu_4\text{-AsCo}_3(\text{CO})_9]_3$, showing the relative orientations of the linked tetrahedra; (b) the conformation of the central As_3Co_3 ring in $[\mu_4\text{-AsCo}_3(\text{CO})_9]_3$.

linking of the metal skeleton and the conformation of the six-membered As_3Co_3 central ring.

Results and discussion

As with the reactions of the group 14 hydrides with iron carbonyls [2], there is a narrow range of conditions under which AsH_3 reacts with $\text{Fe}(\text{CO})_5$ to give tractable products. In hydrocarbon solvent at $110\text{--}125^\circ\text{C}$ for 30 min, $(\mu_3\text{-As})_2\text{Fe}_3(\text{CO})_9$ (**1**) is produced as the only identified product. At temperatures below 100 or above 130°C no more than traces of $(\mu_3\text{-As})_2\text{Fe}_3(\text{CO})_9$ are produced, and use of longer reaction times did not lead to an increase in the yield. Even under optimum conditions the yield of purified **1** is only fair (15%), but it is a marked improvement on the yield (0.2%!) obtained by the only published alternative route [11]. Furthermore, the preparative procedure is quite straightforward, and uses inexpensive starting materials, so $(\mu_3\text{-As})_2\text{Fe}_3(\text{CO})_9$ joins the relatively rare group of reasonably accessible clusters with a *closo*- E_2M_3 core (E = main group, M = transition metal) [6,12*,13*]. A second, unidentified, dichloromethane-soluble product was con-

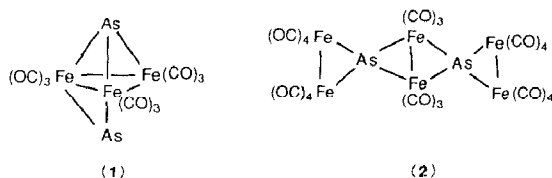
* Reference number with asterisk indicates a note in the list of references.

sistently found in the product mixtures, while the remaining two-thirds of the reaction mixture was insoluble, black material.

This reaction of arsane with $\text{Fe}(\text{CO})_5$ to give a trigonal bipyramidal E_2M_3 cluster directly parallels the corresponding RGeH_3 reactions which gave $(\text{RGe})_2\text{Fe}_3(\text{CO})_9$ under similar conditions, although the yields are better from the germanium hydrides [12a].

We attempted to prepare the corresponding antimony cluster from SbH_3 , but without success; the hydride decomposes to antimony metal above 70°C , yielding only traces of soluble carbonyl-containing material. This is perhaps not surprising in view of the instability of stibane. A more promising route to the antimony analogue may be provided by modification of the three-step, non-hydride route used to synthesise the bismuth analogue $(\mu_3\text{-Bi})_2\text{Fe}_3(\text{CO})_9$ [13c*].

The reaction of AsH_3 with $\text{Fe}_2(\text{CO})_9$ produced a little $(\mu_3\text{-As})_2\text{Fe}_3(\text{CO})_9$, (**1**), while the major soluble product was shown to be $[\text{Fe}_2(\text{CO})_8(\mu_4\text{-As})]_2[\text{Fe}_2(\text{CO})_6]$ (**2**)



by a FAB mass spectrum and an X-ray crystal structural study. Only comparatively weakly diffracting crystals were found so the structural analysis is less precise than usual, but the main features are unambiguous. The overall geometry is shown in Fig. 1, and consists of four linked AsFe_2 triangles. The antimony analogue of **2** has been reported previously by two groups [15,16], prepared by different routes although both involved salt elimination reactions with SbCl_3 . Both groups characterised the compound by X-ray crystallography, although they each isolated different isomorphs, Whitmire et al. [15] obtained red orthorhombic crystals from CH_2Cl_2 , whereas Cowley et al. [16] obtained green monoclinic crystals from hexane. The crystals of the green arsenic compound **2** described in the present work came from hexane, but were isomorphous with the orthorhombic antimony complex.

Selected structural parameters for $[\text{Fe}_2(\text{CO})_8(\mu_4\text{-As})]_2[\text{Fe}_2(\text{CO})_6]$ (**2**) are given in Table 2. The four As–Fe bonds to the outer $\text{Fe}_2(\text{CO})_8$ groups are longer ($2.40(1) \text{ \AA}$) than those to the inner $\text{Fe}_2(\text{CO})_6$ group ($2.34(1) \text{ \AA}$); the same pattern was found for the antimony complex, and was explained in terms of the *spiro* group 15 atom contributing three electrons in the bonds to the inner Fe_2 unit, and two electrons to the outer Fe_2 groups [15,16]. This interpretation is supported by comparison with the isoelectronic and pseudo-isomorphous compounds $[\text{Fe}_2(\text{CO})_8(\mu_4\text{-E})]_2[\text{Fe}_2(\text{CO})_7]$ ($\text{E} = \text{Ge}, \text{Sn}$) which incorporate four-electron *spiro* atoms; here, in contrast, the inner E–Fe bonds are longer than those to the outer $\text{Fe}_2(\text{CO})_8$ groups [2c]. All the Fe–Fe distances in (**2**) are shorter by ca 0.1 \AA than those in the antimony analogue, reflecting the smaller size of the bridging atoms.

For **2** the dihedral angles between the triangles with common As-apices are 86.1 and 84.7° , and that between the two triangles with a common Fe–Fe edge (the butterfly angle) is 109.9° , barely distinguishable from those in the antimony analogue [15,16]. We note the shortest intramolecular non-bonded contact between opposite ends of the molecule is the relatively short O(34) ... O(64) distance of 2.87 \AA , which is similar to the equivalent distance in the antimony species. This steric

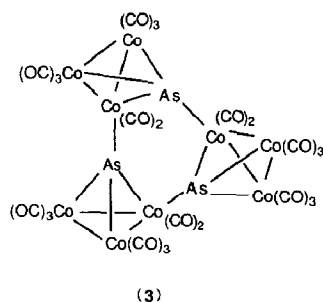
interaction is obviously not especially severe, since the distance would be readily increased by a small opening of the butterfly angle. Again the dihedral angles are in contrast to those in the Ge and Sn species; the Ge compound showed a wide butterfly angle, (132.3°) with near-perpendicular *spiro* angles at the Ge atoms, whereas the Sn compound had a more normal butterfly angle (115.8°) but had one *spiro* angle at Sn of 73.1° [2c]. For the related mixed-metal cluster $[\text{Co}_2(\text{CO})_7(\mu_4\text{-Ge})]_2[\text{Fe}_2(\text{CO})_7]$ the butterfly angle was 111° [1c]. All of these variations suggest that for these 102-electron, linked-triangle E_2M_6 compounds the metal core is quite flexible. The variety of angles arises from the minimisation of interactions between non-bonded carbonyls, and from the packing forces in the particular crystal lattices adopted.

With $\text{Co}_2(\text{CO})_8$, AsH_3 reacts slowly in hexane at room temperature to give $[\mu_4\text{-AsCo}_3(\text{CO})_8]_3$ (**3**) in moderate yields. Even after one month there was unchanged $\text{Co}_2(\text{CO})_8$, and the amount of hydrogen evolved in the reaction suggested that only about a third of the original amount of arsane had reacted. The reaction presumably involves the initial formation of $\mu_3\text{-AsCo}_3(\text{CO})_9$, which then undergoes ready trimerisation, as found previously [8,9] for salt-elimination reactions between AsCl_3 and $[\text{Co}(\text{CO})_4]^-$ or between AsI_3 and $\text{Co}_2(\text{CO})_8$. We note that the recently reported bismuth analogue $\mu_3\text{-BiCo}_3(\text{CO})_9$ does not show this tendency to trimerise [14], presumably reflecting the decreasing basicity of the group 15 atom on descending the Periodic Table.

Attempts to increase the reaction rate and enhance the yields of the arsenic cluster by heating the reaction mixture, were thwarted by the increased conversion of $\text{Co}_2(\text{CO})_8$ to $\text{Co}_4(\text{CO})_{12}$, which is an inevitable side reaction. The preparation of $[\mu_4\text{-AsCo}_3(\text{CO})_8]_3$ by the hydride route therefore offers no advantage over the original preparation involving salt-elimination, although yields are comparable by the two methods.

Again there are parallels between the AsH_3 and RGeH_3 reactions with $\text{Co}_2(\text{CO})_8$, in that germanes give $\text{RGeCo}_3(\text{CO})_9$ as one of the products, corresponding to the $\text{AsCo}_3(\text{CO})_9$ that is presumably the initial product in the arsane system. However germanes also give the partly open cluster $\text{RGe}[\text{Co}(\text{CO})_4]\text{Co}_2(\text{CO})_7$, which does not seem to have an analogue in the AsH_3 reactions.

The cluster $(\mu_4\text{-AsCo}_3(\text{CO})_8)_3$ (**3**) was readily identified by comparison with published spectroscopic data. An earlier (1974) X-ray crystal structure determina-



tion of this trimer has been mentioned [17], but no details have been published in an accessible form. We therefore carried out a full structural characterisation.

The molecule consists of three AsCo_3 tetrahedra linked together in a cycle with the As atom of one unit bonded to a cobalt atom of an adjacent unit (see Fig. 2).

The As atoms are therefore acting as Lewis bases, displacing a CO from the presumed precursor $\mu_3\text{-AsCo}_3(\text{CO})_9$ molecules. (The basicity of arsenic in these clusters is well illustrated by the formation of species such as $(\text{OC})_5\text{CrAsCo}_3(\text{CO})_9$ or $(\text{OC})_4\text{FeAsCo}_3(\text{CO})_9$ [9,18]). There are no indications of any oligomers other than trimers, although there is no obvious reason why tetramers, pentamers etc. should be excluded. Interactions between carbonyl ligands on adjacent units may direct a particular orientation that encourages cyclisation once the chain is three units long. The trimer generates an As_3Co_3 ring at the centre of the structure, and the conformation of this is shown in Fig. 3. Five of the six atoms are approximately coplanar (maximum deviation from a least squares plane less than 0.09 Å) while the sixth, As(2), is 0.75 Å from this plane. The As–Co–As angles are all similar (93–95°) while the Co–As–Co angles are much wider at 141 and 144° for As(1) and As(3), but 134° for the out-of-plane As(2). These features presumably arise because of the need to combine three sterically demanding units. The As–Co bonds all fall within a narrow range of 2.265(5)–2.307(5) Å, with those between tetrahedra appearing marginally shorter than those within an AsCo_3 unit, while the Co–Co bond lengths are between 2.546 and 2.599 Å. These bond lengths are in complete agreement with those in cluster such as $(\text{OC})_5\text{CrAsCo}_3(\text{CO})_9$ or $(\text{OC})_9\text{Co}_3\text{AsCo}_4(\text{CO})_{11}$ [18].

The experiments reported in this paper show that reactions with AsH_3 provide a practicable route to arsenic-containing clusters, although the yields are only moderate. There are some parallels between the reactions of AsH_3 and RGeH_3 with metal carbonyls, and the formation of $[\text{Fe}_2(\text{CO})_8(\mu_4\text{-As})]_2[\text{Fe}_2(\text{CO})_6]$ from AsH_3 and $\text{Fe}_2(\text{CO})_9$ is directly comparable to the production of $[\text{Co}_2(\text{CO})_7(\mu_4\text{-Ge})]_2[\text{Co}_2(\text{CO})_6]$ from GeH_4 and $\text{Co}_2(\text{CO})_8$ [1b]. By using As in place of Ge, and Fe in place of Co, we can expect to encounter more pseudo-isoelectronic comparisons of this type.

Acknowledgements

We thank Dr. Ward T. Robinson, University of Canterbury, for collection of X-ray intensity data, Professor M.I. Bruce, University of Adelaide, for FAB mass spectra, and the New Zealand Universities Grants Committee for financial support.

References

- (a) R.F. Gerlach, K.M. Mackay and B.K. Nicholson, *J. Chem. Soc., Dalton Trans.*, (1981) 80; (b) S.P. Foster, K.M. Mackay and B.K. Nicholson, *Inorg. Chem.*, 24 (1985) 909; (c) S.G. Anema, K.M. Mackay, L.C. McLeod, B.K. Nicholson and J.M. Whittaker, *Angew. Chem. Int. Ed. Eng.*, 25 (1986) 759; (d) K.M. Mackay, B.K. Nicholson, A.W. Sims and C.C. Tan, *Acta Crystallogr., C*, 43 (1987) 633; (e) M. Van Tiel, K.M. Mackay and B.K. Nicholson, *J. Organomet. Chem.*, 326 (1987) C101.
- (a) S.G. Anema, G.C. Barris, K.M. Mackay and B.K. Nicholson, *J. Organomet. Chem.*, 350 (1988) 207; (b) S.G. Anema, K.M. Mackay and B.K. Nicholson, *ibid.*, 372 (1989) 25; (c) S.G. Anema, K.M. Mackay and B.K. Nicholson, *Inorg. Chem.*, 28 (1989) 3158;
- See for example E. Rottinger and H. Vahrenkamp, *J. Organomet. Chem.*, 213 (1981) 1; K. Natarajan, O. Scheidsteiger and G. Huttner, *ibid.*, 221 (1981) 301.
- Guldner, B.F.G. Johnson, J. Lewis and A.D. Massey, XIIIth Intern. Conf. Organomet. Chem., Torino, 1988, Abstract 391.
- F.A. Cotton and G. Wilkinson, *Advanced Inorganic Chemistry*, Wiley, New York, 1980.

- 6 W.A. Herrmann, *Angew. Chem. Int. Ed. Eng.*, 25 (1986) 56; K.H. Whitmire, *J. Coord. Chem.*, 17 (1988) 95.
- 7 W. Jolly and J. Drake, *Inorganic Synth.*, 7 (1963) 34.
- 8 A. Vizi-Orosz, V. Galamb, G. Palyi, L. Marko, G. Bor and G. Natile, *J. Organomet. Chem.*, 107 (1976) 235.
- 9 A. Vizi-Orosz, V. Galamb, G. Palyi and L. Marko, *J. Organomet. Chem.*, 216 (1981) 105.
- 10 G.M. Sheldrick, SHELXS-86, A Program for Solving Crystal Structures, University of Gottingen, 1986; SHELX-76, A Program for Crystal Structure Determination, University of Cambridge, 1976.
- 11 L.T. Delbaere, L.J. Kruczynski and D.W. McBride, *J. Chem. Soc., Dalton Trans.*, (1973) 307.
- 12 For group 14 examples see: S.G. Anema, K.M. Mackay and B.K. Nicholson, *Organometallics*, submitted; H.J. Haupt, A. Gotze and U. Florke, *Z. Anorg. Allg. Chem.*, 557 (1988) 82; H.J. Haupt and U. Florke, *Acta Crystallogr., C*, 44 (1988) 472; J.T. McNeese, S. Wreford, L.D. Tipton and R. Bau, *J. Chem. Soc., Chem. Commun.*, (1977) 390; D. Lentz and H. Michael, *J. Organomet. Chem.*, 372 (1984) 109. D. Lentz and H. Michael, *Inorg. Chem.*, 28 (1989) 3396.
- 13 For group 15 examples see: (a) H. Lang, G. Huttner, L. Zsolnai, G. Mohr, B. Sigwarth, U. Weber, O. Orama and I. Jibril, *J. Organomet. Chem.*, 304 (1986) 157; (b) M.R. Churchill, J.C. Fettinger and K.H. Whitmire, *ibid.*, 284 (1985) 13; (c) C. Hay, B.F.G. Johnson, J. Lewis, P.R. Raithby and A.J. Whitton, *J. Chem. Soc., Dalton Trans.*, (1988) 2091. A recent group 16 example is in J.R. Lockemeyer, T.B. Rauchfuss and A.L. Rheingold, *J. Am. Chem. Soc.*, 111 (1989) 5733.
- 14 K.H. Whitmire, J.S. Leigh and M.E. Gross, *J. Chem. Soc., Chem. Commun.*, (1987) 926; S. Martinengo and G. Ciani, *ibid.*, (1987) 1589.
- 15 A.L. Rheingold, S.J. Geib, M. Shieh and K.H. Whitmire, *Inorg. Chem.*, 26 (1987) 463.
- 16 A.M. Arif, A.H. Cowley and M. Pakulski, *J. Chem. Soc., Chem. Commun.*, (1987) 623.
- 17 R.S. Gall, A.S. Foust, P.J. Pollick, A. Wojcicki and L.F. Dahl, *Abstr. Am. Crystallogr. Meeting*, Berkeley, California, 1974, quoted in ref. 8.
- 18 H. Lang, G. Huttner, B. Sigwarth, I. Jibril, L. Zsolnai and O. Orama, *J. Organomet. Chem.*, 304 (1986) 137.